Effects of Introduction of Hydrophobic Group on Ribavirin Base on Mutation Induction and Anti-RNA Viral Activity

Kei Moriyama,*[,†,⊥] Tetsuya Suzuki,[‡] Kazuo Negishi,[‡] Jason D. Graci,[§] Corinne N. Thompson,[§] Craig E. Cameron,[§] and Masahiko Watanabe[†]

Shujitsu University, School of Pharmacy, Nishigawara, Okayama 703-8516, Japan, Department of Genomics and Proteomics, Okayama University Advanced Science Research Center, Tsushima, Okayama 700-8530, Japan, and Department of Biochemistry and Molecular Biology, The Pennsylvania State University, University Park, Pennsylvania 16802

Received August 9, 2007

One of the possible mechanisms of antiviral action of ribavirin (1-β-D-ribofuranosyl-1,2,4-triazole-3-carboxamide, **1**) is the accumulation of mutations in viral genomic RNA. The ambiguous incorporation of 5′-triphosphate of ribavirin (RTP, **8**) by a viral RNA-dependent RNA polymerase (RdRp) is a key step of the mutation induction. We synthesized three ribavirin analogues that possess hydrophobic groups, 4-iodo-1-β-D-ribofuranosylpyrazole-3-carboxamide (**7a**), 4-propynyl-1-β-D-ribofuranosylpyrazole-3-carboxamide (**7b**), and 4-phenylethynyl-1-β-D-ribofuranosylpyrazole-3-carboxamide (**7c**), and the corresponding triphosphates (**9a**, **9b**, and **9c**, respectively). Steady-state kinetics analysis of the incorporation of these triphosphate analogues by a poliovirus RdRp, $3D^{pol}$, revealed that while the incorporation efficiency of **9a** was comparable to RTP, **9b** and **9c** showed lower efficiency than RTP. Antipolioviral activity of **7a** and **7b** was much more moderate than ribavirin, and **7c** showed no antipolioviral activity. Effects of substituting groups on the incorporation efficiency by $3D^{pol}$ and a strategy for a rational design of more active ribavirin analogues are discussed.

Introduction

Ribavirin (1-β-D-ribofuranosyl-1,2,4-triazole-3-carboxamide, **1**) is a guanosine analogue that has broad-spectrum anti-RNA viral activity. It has been clinically used in combination with interferon α against hepatitis C virus (HCV) infection. Since the discovery of ribavirin in 1972,[1,2] several mechanisms for the antiviral activity have been reported. After uptake into a host cell, ribavirin is metabolized to ribavirin 5′-monophosphate (RMP[a]) by a cellular adenosine kinase. It has been shown that RMP inhibits an inosine monophosphate dehydrogenase (IMDPH) in a host cell.[3,4] Further phosphorylation of RMP by cellular nucleotide kinases yields ribavirin 5′-diphosphate and ribavirin 5′-triphosphate (RTP). It has also been reported that RTP inhibits viral RNA polymerases[5] and that viral RNA transcription is suppressed by producing defective 5′-cap structures containing RTP.[6] These inhibitory actions of ribavirin metabolites on cellular or viral enzymes have been considered to be related to the antiviral action of ribavirin.

Recently, another mechanism of ribavirin antiviral action is reported. Ribavirin is a viral mutagen.[7] Exceeding an error threshold by the accumulation of mutation in viral genomic RNA leads to virus population extinction. This is so-called the lethal mutagenesis or error catastrophe.[8,9] The base moiety of ribavirin, 1,2,4-triazole-3-carboxamide, can base-pair with both cytosine (C) and uracil (U) by a rotation of the carboxamide group (Figure 1).[7] Poliovirus RNA-dependent RNA polymerase ($3D^{pol}$) incorporates RTP opposite both C and U in template RNA. This

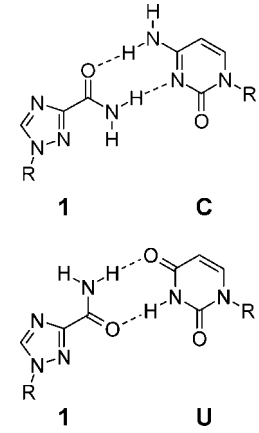

Figure 1. Ambiguous base pairing of ribavirin (**1**) with cytosine (C) and uracil (U). R is ribose.

ambiguous incorporation of RTP by a viral RNA polymerase is a key step of the mutation induction by ribavirin. Therefore, investigation of the structure–activity relation between RTP derivatives and their incorporation by viral RdRp is important to design more potent antiviral drugs derived from ribavirin.

It is reported that providing a hydrophobic property on the base moiety of nucleoside 5′-triphosphate improves its incorporation efficiency by DNA polymerase.[10] Introduction of a propynyl group to dPaTP, an unnatural deoxyribonucleoside 5′-triphosphate, elevated the incorporation efficiency opposite the partner unnatural base, Q on template. Base recognition by DNA polymerase was decreased when a propynyl group was introduced on the Pa base because the incorporation efficiency was increased evenly opposite all types of the template base. Introduction of a hydrophobic propynyl group on base moiety of the triphosphate results in high incorporation efficiency and low base recognition. These properties could be advantageous for the mutation induction. Thus, we hypothesized that by introducing a hydrophobic substitution such

* To whom correspondence should be addressed. Phone: +81-88-665-2126. Fax: +81-88-665-5392. E-mail: k_moriyama@research.otsuka.co.jp.
† Shujitsu University.
⊥ Present address: Otsuka Pharmaceutical Co., Ltd., Hiraishi Ebisuno, Kawauchi-cho, Tokushima 771-0182, Japan.
‡ Okayama University.
§ The Pennsylvania State University.

[a]Abbreviations: RTP, ribavirin 5′-triphosphate; RMP, ribavirin 5′-monophosphate; RdRp, RNA-dependent RNA polymerase.

10.1021/jm7009952 CCC: $40.75
Published on Web 12/08/2007

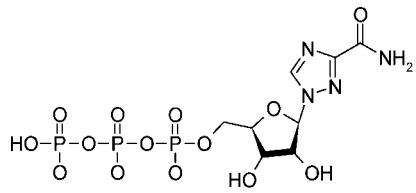

8

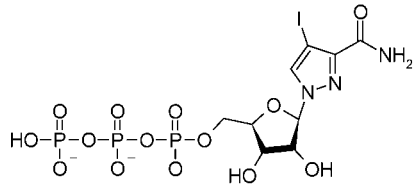

9a

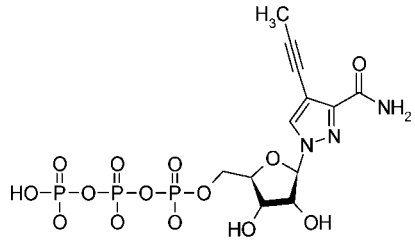

9b

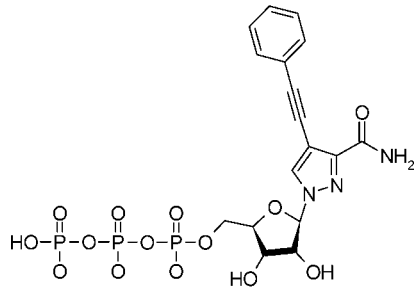

9c

Figure 2. Structures of RTP (**8**) and hydrophobic RTP analogues (**9a**−**c**).

as propynyl group on a ribavirin base, the mutagenicity would become higher than ribavirin, which would lead to an increase of anti-RNA viral activity of ribavirin.

Here, we report chemical syntheses of RTP analogues that possess hydrophobic groups on the base moiety (Figure 2) and their incorporation efficiency by $3D^{pol}$, and the effects of introduction of these substituting groups on the activity of ribavirin are discussed.

Results

Chemical Synthesis. All synthetic pathways are summarized in Scheme 1. Iodination of pyrazole and its derivatives has been carried out previously by boiling them with iodine and potassium iodide in alkaline aqueous solution.[13,18] To accomplish this in milder conditions, we applied a trifluoroacetic acid catalyzed iodination with *N*-iodosuccinimide[11] for iodination of methyl pyrazole-3-carboxylate. Methyl 4-iodopyrazole-3-carboxylate (**5**) was obtained in a sufficient yield (87%), and an iodine substitution at position 4 of the pyrazole ring was confirmed by the disappearance of the H4 signal on ^{1}H NMR (data not shown). Coupling of **5** and protected β-D-ribose was successful using the procedure reported by Manfredini et al.[12] with a minor modification. We found that the coupling product (**6a**) was obtained in better yield (92%) with a smaller amount of byproduct when the reaction was performed at room temperature instead of under reflux conditions as described in the literature.[12] Palladium-catalyzed coupling reactions (**6a** to **6b** and **6c**) and the conversion of nucleosides to its corresponding 5′-triphosphates were carried out as described previously.[10,19] This coupling reaction is very important because various ribavirin analogues as well as **6b** and **6c** can be synthesized from **6a** by the palladium-catalyzed reaction. **6a** could be a key intermediate for synthesizing ribavirin analogues. Hydrophobicity of RTP and RTP analogues (**9a**−**c**) was evaluated from these retention times (t_R) from reverse-phase HPLC analyses under HPLC condition II (see Experimental Section). The t_R values of these triphosphates are listed in Table 1. The order of hydrophobicity was RTP < **9a** = **9b** < **9c**.

Incorporation Efficiency of Hydrophobic Ribavirin 5′-Triphosphate Analogues by Poliovirus RNA Dependent RNA Polymerase, $3D^{pol}$. Ribavirin can form base pairs with both C and U by the rotation of carboxamide group (Figure 1),[7] and this results in the ambiguous incorporation of ribavirin 5′-triphosphate (RTP, **8**), an intracellular metabolite of ribavirin, opposite template C and U by $3D^{pol}$. Consequently, ribavirin induces mutation on viral genomic RNA and causes error catastrophe.[7−9] The incorporation assay of RTP (**8**) and its analogues (**9a**−**c**) opposite C and U by $3D^{pol}$ was performed with a template primer called "sym/sub-C" and "sym/sub-U", respectively (Figure 3).[7] First, 5′-triphosphates (**8**, **9a**−**c**) were applied to time course analysis of $3D^{pol}$ incorporation with sym/sub-U and sym/sub-C (Figure 4). Incorporation of iodinated RTP analogue (**9a**) and propynyl RTP analogue (**9b**) was slower than that of RTP opposite template C (Figure 4A). No elongated product was observed for phenylethynyl RTP analogue (**9c**) on sym/sub-C. In contrast, opposite U, the incorporation time course of **9a** was almost identical with that of RTP (**8**) (Figure 4B). **9b** was incorporated slightly more slowly than **9a**, and **9c** was rarely incorporated opposite U as well as opposite C. To evaluate these incorporation efficiencies, steady-state kinetics analyses were carried out. Results are summarized in Table 2, and the incorporation efficiencies (k_{cat}/K_M) of 5′-triphosphates opposite C and U are shown in the bar graph (Figure 5). k_{cat}/K_M of **9a** opposite U was 2.0×10^{-5} (μM^{-1} s^{-1}), ~2-fold larger than that of RTP (**8**) (1.1×10^{-5} (μM^{-1} s^{-1})). On the other hand, k_{cat}/K_M of **9a** opposite C (4.4×10^{-6} (μM^{-1} s^{-1})) was ~2-fold smaller than that of RTP (8.4×10^{-6} (μM^{-1} s^{-1})). These results indicate that **9a** is comparable to RTP in its potential to be incorporated into viral genomic RNA. The K_M values of **9a** on both sym/sub-C and sym/sub-U were smaller than that of RTP, which indicates that **9a** was superior to RTP in the affinities with sym/sub-$3D^{pol}$ complexes. **9b** showed almost equal incorporation efficiency to RTP opposite U but ~3-fold less than RTP opposite C. **9c** provides no detectable elongated product. Although kinetic parameters of correct NTP incorporations (GTP on sym/sub-C and ATP on sym/sub-U) were not determined because of rapid reactions with these template−NTP combinations in our experimental condition, we can refer to previously reported pre-steady-state kinetics data on the same sym/sub-C and sym/sub-U, which revealed that RTP incorporation by $3D^{pol}$ was 3×10^5 fold slower than GTP incorporation opposite C[7] and 2×10^4 fold slower than ATP incorporation opposite U.[20]

Scheme 1. Chemical Synthesis of Hydrophobic Ribavirin Analogues (**7a**−**c**) and RTP Analogues (**9a**−**c**) .[a]

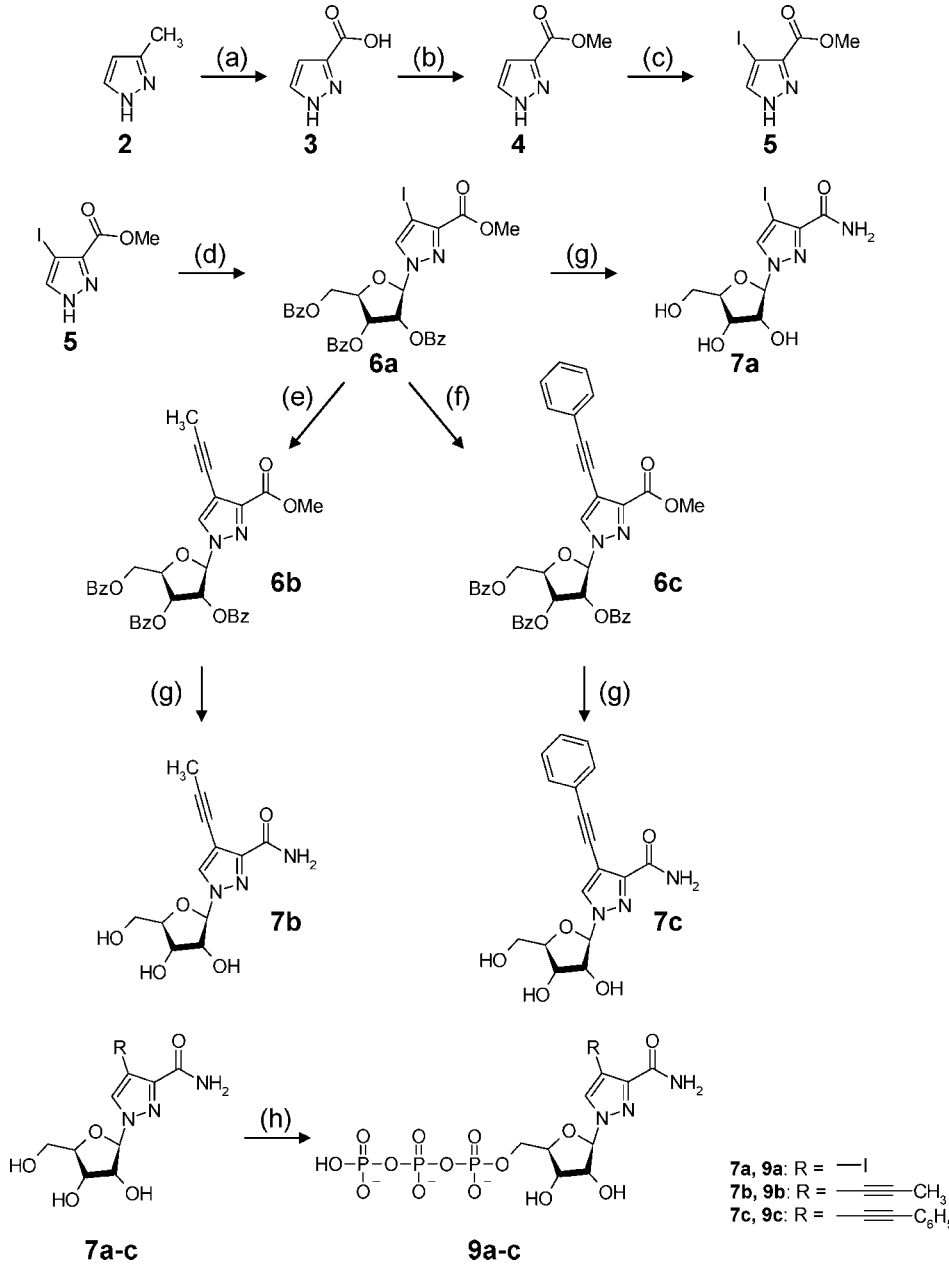

[a] Reagents and conditions: (a) $KMnO_4$, H_2O, reflux; (b) H_2SO_4, MeOH, room temp; (c) *N*-iodosuccinimide, trifluoroacetic acid, CH_3CN, room temp; (d) β-D-ribofuranose-1-acetate-2,3,5-tribenzoate, 1,1,1,3,3,3-hexamethyldisilazane, $(NH_4)_2SO_4$, Me_3SiCl, CF_3SO_3H, CH_3CN, room temp; (e) $Pd(PPh_3)_4$, CuI, Et_3N, tributyl(1-propynyl)tin, room temp; (f) $Pd(PPh_3)_4$, CuI, Et_3N, ethynylbenzene, room temp; (g) NH_3, MeOH, room temp; (h) (1) $POCl_3$, Proton Sponge, $(CH_3O)PO$, 0°C, (2) tri-*n*-butylamine, bis(tri-*n*-butylammonium)pyrophosphate, DMF, 0°C.

Table 1. Retention Times of RTP (**8**) and Hydrophobic RTP Analogues (**9a**−**c**) on Reverse-Phase HPLC

NTP	retention time (min)[a]
8	7.71
9a	10.56
9b	10.14
9c	16.68

[a] Retention time from HPLC condition II (see Experimental Section). Wavelength for detection varied with 5′-triphosphates: 220, 250, 260, and 271 nm for **8**, **9a**, **9b**, and **9c**, respectively.

A

5'-GAUCGGGCCC-3'

3'-CCCGGGCUAG-5'

B

5'-GCAUGGGCCC-3'

3'-CCCGGGUACG-5'

Figure 3. Sym/sub-C (A) and sym/sub-U (B). Underlined bases were the templating bases for $3D^{pol}$ assays.

Antipolioviral Activities of Hydrophobic Ribavirin Analogues. Antipolioviral activities of ribavirin (**1**) and hydrophobic analogues (**7a**−**c**) were tested, and results were summarized in Table 3. Each compound was applied to poliovirus infected HeLa cells at the final concentrations of 0.5 and 2 mM in culture medium. Iodine- and propynyl-substituted ribavirin analogues (**7a** and **7b**, respectively) showed very moderate antipolioviral

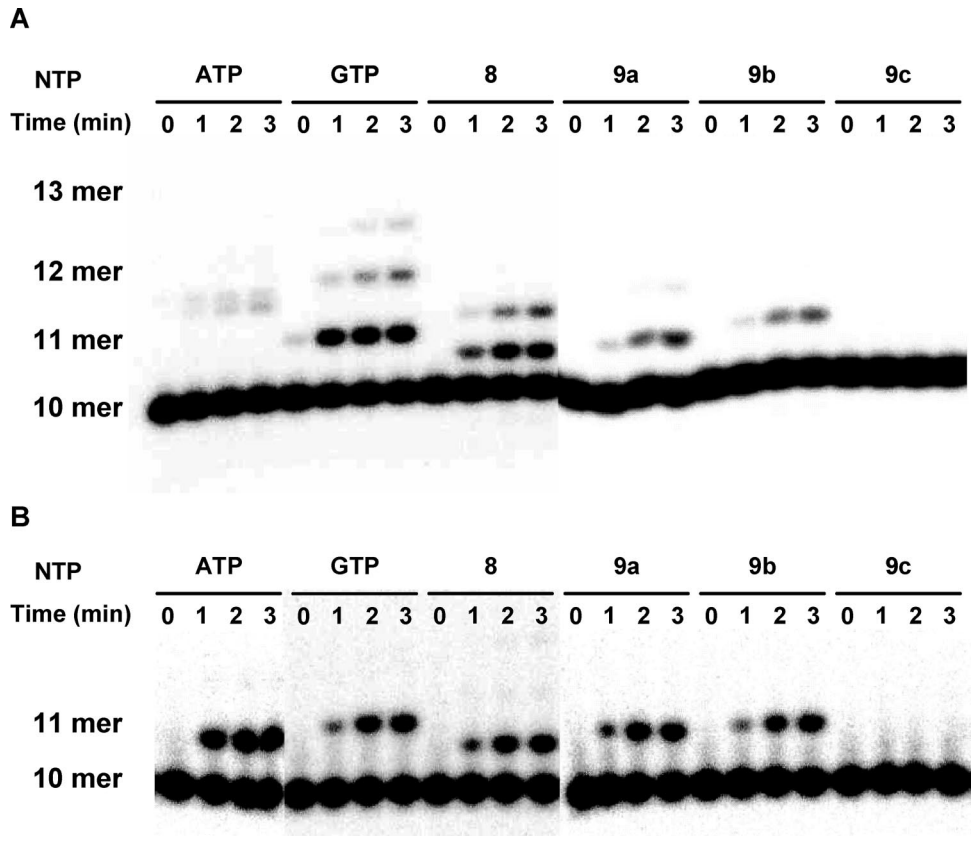

Figure 4. Incorporation of 5′-triphosphates by $3D^{pol}$ into ^{32}P-labeled sym/sub-C (A) and sym/sub-U (B) templates. Products of $3D^{pol}$ assays were separated by 20% polyacrylamide denaturing gel electrophoresis and visualized by Personal Molecular Imager FX (Bio-Rad).

Table 2. Kinetic Parameters for Incorporation of RTP (**8**) and Hydrophobic RTP Analogues (**9a**−**c**) by $3D^{pol}$ [a]

NTP	K_M (μM)	k_{cat} ($\times 10^{-4}$) (s^{-1})	k_{cat}/K_M ($\times 10^{-6}$) ($\mu M\ s^{-1}$)
sym/sub-C			
ATP	110 ± 30[b]	0.82 ± 0.11	0.74
8	69 ± 18	5.8 ± 0.9	8.4
9a	40 ± 5	1.8 ± 0.2	4.4
9b	51 ± 16	1.3 ± 0.3	2.6
9c	nd[c]	nd[c]	nd[c]
sym/sub-U			
GTP	56 ± 20	5.0 ± 1.1	8.9
8	34 ± 9	3.7 ± 0.3	11
9a	24 ± 2	4.7 ± 0.7	20
9b	35 ± 6	3.1 ± 0.6	9.1
9c	nd[c]	nd[c]	nd[c]

[a] Initial rate of reaction was determined as {(band intensity of ≥11-mer)/[(band intensity of ≥11-mer) + (band intensity of 10-mer)]}(0.5/120) ($\mu M\ s^{-1}$) for each concentration of NTP. k_{cat} and K_M values were calculated from Lineweaver–Burk plot. [b] Mean ± standard deviation ($n = 3$). [c] No elongated product was detected.

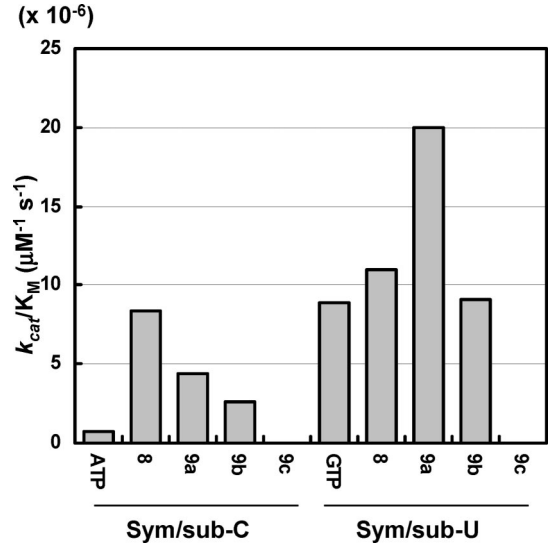

Figure 5. Incorporation efficiencies (k_{cat}/K_M from steady-state kinetics) of RTP and analogues into sym/sub-C and sym/sub-U.

activity when compared to ribavirin. No antipolioviral effect was observed on phenylethynyl-substituted ribavirin analogue (**7c**).

Discussion

On the basis of the observation that a substitution by a hydrophobic group on the base moiety of dNTP results in an increase of the incorporation efficiency accompanied with a decrease of base recognition by DNA polymerase,[10] we designed ribavirin 5′-triphosphate analogues that possessed hydrophobic groups on the base to attempt to increase the rate of mutation induction. We synthesized iodine-, propynyl-, and phenylethynyl-substituted ribavirin analogues (**7a**, **7b**, and **7c**, respectively) and the corresponding 5′-triphosphates (**9a**, **9b**, and **9c**, respectively). Steady-state kinetics of RTP and **9a**−**c** incorporation by purified poliovirus RdRp, $3D^{pol}$ revealed that the incorporation efficiencies of **9a** opposite C and U were ∼2-fold lower and ∼2-fold higher, respectively, than RTP (Table 2 and Figure 5). This indicates that **9a** is comparable to RTP in terms of in vitro incorporation into viral genomic RNA.

Judging from the retention time on HPLC, the hydrophobicities of synthesized 5′-triphosphates increased in the order of RTP < **9a** = **9b** < **9c** (Table 1). Contrary to our expectation, the incorporation efficiencies by $3D^{pol}$ were decreased in the

Table 3. Antipolioviral Activity of Ribavirin (**1**) and Hydrophobic Ribavirin Analogues (**7a**−**c**)

nucleoside	relative PFU (%)[a]
none	100
1 (0.5 mM[b])	40
1 (2 mM)	4
7a (0.5 mM)	76
7a (2 mM)	68
7b (0.5 mM)	94
7b (2 mM)	57
7c (0.5 mM)	122
7c (2 mM)	91

[a] Virus titer after 6 h of infection in the presence of nucleosides compared to an untreated control (defined as 100%). The standard deviation of each titer is typically less than 40% based on our prior experiments. [b] Final concentration in culture medium.

order of RTP = **9a** > **9b** > **9c** (Table 2 and Figure 5). This contrasts with a finding on DNA polymerase (Klenow fragment of DNA polymerase I) incorporation of dNTP analogues.[10] This difference of the behavior of hydrophobic 5′-triphosphate between DNA and RNA polymerase might be explained from the structure of polymerases. The crystal structure of the Klenow fragment[21] revealed that the base of incoming dNTP interacts with aromatic amino acids, His881 or Tyr766. This means that the interaction between the base of dNTP and polymerase active site is dependent on $\pi-\pi$ interaction. Since a propynyl substitution on the base expands the distributing area of the π electron, $\pi-\pi$ interaction of dNTP and polymerase would be increased and thus the incorporation efficiency of a propynyl substituted dNTP becomes higher. In contrast, the base of incoming NTP interacts with Arg174 of the polymerase active site of poliovirus $3D^{pol}$ by cation$-\pi$ interaction.[22,23] One of the possible mechanisms for the decrease in the incorporation efficiency by propynyl and phenylethynyl substitution is that a substitution with these electron-withdrawing groups (the electronegativity of these groups is ∼3.0)[24] would reduce the π electron density of the base and that cation$-\pi$ interaction between **9b** or **9c** and $3D^{pol}$ would be weakened. As a result, the affinity of these 5′-triphosphates and $3D^{pol}$ is decreased. 1-β-D-Ribofuranosyl-3-nitropyrrole 5′-triphosphate (3-NPNTP) also showed much lower incorporation efficiency than RTP.[17] The same mechanism could be underlying this observation because a nitro group is a strong electron-withdrawing group. As for iodine substitution, since the electronegativity of iodine is 2.5, which is the same as that of carbon, the substituted iodine behaves as an electron-donating group because of the electron-donating resonance effect (+R effect) of lone pair electrons on iodine, enriches π electron density of pyrazole ring, and strengthens cation$-\pi$ interaction. It is possible that the decrease of the K_M value of **9a** compared with RTP arises from this effect. Beyond the electronic contributions, the bulkiness of the substituting group could greatly affect the incorporation efficiency of RTP analogues. The phenylethynyl group might be too bulky to fit the active site structure of $3D^{pol}$. Taking all these effects into consideration, the introduction of a substituting group on the ribavirin base such as a small and electron-donating group might be more effective to increase incorporation efficiency by $3D^{pol}$. We are now trying to seek novel RTP analogues that possess more potent mutagenicity on the basis of findings in this work.

Antipolioviral activity of ribavirin and analogues (**1**, **7a**−**c**) was not wholly consistent with the incorporation efficiency of the corresponding 5′-triphosphates (**8**, **9a**−**c**) judged from steady-state kinetics of incorporation by $3D^{pol}$ in vitro (Table 2 and Figure 5). While **9a** showed in vitro incorporation efficiency comparable to RTP as described above, antipolioviral activity of **7a** was much lower than that of ribavirin (Table 3). A reason for this difference is the mutagenicity of **9a**. One factor that might influence mutagenicity is if the substitution affects rotation of the carboxamide group due to steric or electronic hindrance since the mutagenic property of ribavirin is based on this rotation.[7] The incorporation efficiency of **9a** is better than ribavirin opposite U, and **9b** is about the same as ribavirin in that context. However, both are worse than ribavirin in the context of a templating C. This suggests that the analogues might favor the "A-like" form and that the "G-like" form might be less prevalent. It is possible that the substitution of position 4 of the ribavirin base makes the "A-form" more stable and the "G-form" less stable. Thus, even if they are incorporated efficiently, they may not induce mutation at a high enough rate to show activity in the antiviral assay. Another reason for the low antipolioviral activity of **7a** is that it might be poorly phosphorylated in the infected cells. Ribavirin is phosphorylated by cytosolic 5′-nucleotidase II as well as adenosine kinase.[25] It is necessary for ribavirin analogues to be phosphorylated intracellularly by these enzymes to behave as a viral mutagen. Investigation of the structure–activity relation between ribavirin analogues and phosphorylation activity of these enzymes as well as the property of rotation of the carboxamide group should garner further attention.

A rational design of RTP analogues that aims to increase the incorporation efficiency and the mutation induction ability from the viewpoint of NTP and polymerase interaction in the active site may be a useful strategy for discovering ribavirin analogues that are more active against RNA viruses. In parallel, rotation of the carboxamide group and intracellular phosphorylation of the analogues must be studied precisely to understand the antiviral and mutagenic properties of ribavirin analogues in the infected cells.

Experimental Section

General Procedures. ^{1}H, ^{13}C, and ^{31}P NMR. Spectra were recorded on ECA500 spectrometer with Delta software (JEOL). Except where noted, the temperature for NMR measurement was 25 °C.

High-Resolution Mass Spectra (HR-MS). HR-MS were obtained on MicroTOF LC (Bruker Daltonics). Spectra were calibrated with an internal standard "Tune Mix solution" (Bruker Daltonics).

Ultraviolet–Visible Spectra. UV–vis spectra for synthesized 5′-triphosphates over the range 220−400 nm were recorded on GE Healthcare Ultrospec 1100 pro.

Silica Gel Column Chromatography. Chromatography was performed on Wakogel C-200 (Wako). Solvents were described in each procedure.

HPLC. HPLC data were collected from a JASCO HPLC system (HPLC pump, PU-2089Plus; UV detector, UV-2075Plus) with HSS-2000 software. HPLC condition I is as follows: column, SymmetryPrep C_{18} 7 μm (column size ∅ 19 mm × 150 mm, Waters); solvent A, H_2O; solvent B, 50% (v/v) CH_3CN in H_2O; 0–10 min, 0–100% B; 10–15 min, 100% B; 15–16 min, 100–0% B; 16–21 min, 0% B; flow rate, 10 mL/min; detection, UV 254 nm. HPLC condition II is as follows: column, Cosmosil 5C_{18}-MS-II (column size ∅ 4.6 mm × 250 mm, Nacalai tesque); solvent A, 100 mM tetraethylammonium acetate (TEAA) in H_2O; solvent B, 100 mM TEAA and 50% (v/v) CH_3CN in H_2O; 0–15 min, 0–60% B; 15–16 min, 60–100% B; 16–21 min, 100% B; 21–22 min, 100–0% B; 22–27 min, 0% B; flow rate, 1 mL/min. HPLC condition III is as follows: column, Cosmosil 5C_{18}-MS-II (column size ∅ 4.6 mm × 250 mm, Nacalai tesque); solvent A, 100 mM TEAA in H_2O; solvent B, 100 mM TEAA and 50% (v/v) CH_3CN in H_2O; 0–15

min, 0–100% B; 15–20 min, 100% B; 20–21 min, 100–0% B; 21–26 min, 0% B; flow rate, 1 mL/min.

All synthetic reactions were monitored by thin layer chromatography (TLC) with silica gel sheet 60 F_{254} (Merck).

Ribavirin (1-β-D-ribofuranosyl-1,2,4-triazole-3-carboxamide, 1). Ribavirin (**1**) was synthesized and crystallized according to the literature.[2] ^{1}H NMR (500 MHz, DMSO-d_6) δ (ppm) 8.83 (s, 1H), 7.79 (bs, 1H), 7.58 (bs, 1H), 5.78 (d, 1H, J = 3.4 Hz), 5.53 (d, 1H, J = 4.6 Hz), 5.15 (d, 1H, J = 4.6 Hz), 4.87 (t, 1H, J = 5.5 Hz), 4.32 (q, 1H, J = 4.4 Hz), 4.10 (q, 1H, J = 5.0 Hz), 3.91 (q, 1H, J = 4.4 Hz), 3.62–3.57 (m, 1H), 3.49–3.44 (m, 1H).

Methyl Pyrazole-3-carboxylate (4). Methyl pyrazole-3-carboxylate (**4**) was synthesized by oxidation of 3-methylpyrazole (**2**) followed by ester formation. Briefly, to a solution of 4.11 g (50.0 mmol) of 3-methylpyrazole (Tokyo Kasei) in 150 mL of H_2O was added slowly 17.38 g (110 mmol) of $KMnO_4$ in 100 mL of H_2O, and the solution was heated to reflux conditions for 4 h. After the reaction mixture was cooled to room temperature, insoluble material was removed by filtration. The filtrate was evaporated to ~30 mL, and then pyrazole-3-carboxylic acid (**3**) (2.68 g, 23.9 mmol, 48%) was crystallized by adding concentrated HCl to give pH ~2. To a solution of 2.04 g (18.2 mmol) of **3** in 36 mL of dry methanol was added 2.9 mL (54.4 mmol) of H_2SO_4, and the solution was stirred at room temperature overnight under an argon atmosphere. The solution was evaporated, and the residue was dissolved in 50 mL of H_2O. $NaHCO_3$ was added to neutralize. The solution was extracted with EtOAc, dried over Na_2SO_4, filtrated, and evaporated. An amount of 2.00 g (15.9 mmol, 87%) of **4** was obtained by silica gel chromatography (solvent, 5−10% methanol in CH_2Cl_2) as a white solid. ^{1}H NMR (500 MHz, DMSO-d_6, 55 °C) δ (ppm) 13.40 (bs, 1H), 7.75 (bs, 1H), 6.72 (s, 1H), 3.78 (s, 3H).

Methyl 4-Iodopyrazole-3-carboxylate (5). An efficient iodination of aromatic compounds in mild conditions is reported by Castanet et al.[11] According this procedure, **4** was converted to the 4-iodinated form **5**. Amounts of 1.74 g (13.8 mmol) of **4** and 3.41 g (15.2 mmol) of *N*-iodosuccinimide were dissolved in 55 mL of dry CH_3CN under argon atmosphere. To the stirring solution, 320 μL (4.14 mmol) of trifluoroacetic acid was added, and the solution was stirred for 3 h. After evaporation, the residue was partitioned with EtOAc/5% $NaHCO_3$. The organic layer was dried over Na_2SO_4, filtrated, and evaporated. **5** (3.03 g, 12.0 mmol, 87%) was crystallized from *n*-hexane/EtOAc. ^{1}H NMR (500 MHz, DMSO-d_6, 55 °C) δ (ppm) 13.74 (bs, 1H), 7.98 (bs, 1H), 3.79 (s, 3H).

Methyl 4-Iodo-1-(2′,3′,5′-tribenzoyl-β-D-ribofuranosyl)pyrazole-3-carboxylate (6a). A coupling reaction of **5** and sugar moiety was carried out according to the literature[12] with minor modifications. To a solution of 2.91 g (11.5 mmol) of **5** in 115 mL of dry CH_3CN was added 8.74 g (17.3 mmol) of β-D-ribofuranose 1-acetate 2,3,5-tribenzoate (Tokyo Kasei), 2.68 mL (12.7 mmol) of 1,1,1,3,3,3-hexamethyldisilazane, and 152 mg (1.15 mmol) of ammonium sulfate under argon atmosphere, and the solution was stirred at room temperature. An amount of 1.76 mL (13.9 mmol) of chlorotrimethylsilane followed by 2.45 mL (27.7 mmol) of trifluoromethanesulfonic acid was added, and the solution was stirred at room temperature for 3 h. Mixed with 115 mL of CH_2Cl_2, the solution was washed with saturated $NaHCO_3$ aqueous solution. The organic layer was subsequently washed with saturated NaCl aqueous solution, dried over Na_2SO_4, filtrated, and evaporated. An amount of 7.38 g (10.6 mmol, 92%) of **6a** was obtained by silica gel column chromatography (solvent, *n*-hexane/EtOAc = 4: 1 (v/v)). ^{1}H NMR (500 MHz, $CDCl_3$) δ (ppm) 8.05 (d, 2H, J = 6.9 Hz), 7.97 (d, 2H, J = 6.9 Hz), 7.92 (d, 2H, J = 6.9 Hz), 7.81 (s, 1H), 7.59–7.53 (m, 3H), 7.45 (t, 2H, J = 7.7 Hz), 7.40 (t, 2H, J = 8.0 Hz), 7.36 (t, 2H, J = 7.7 Hz), 6.26 (d, 1H, J = 2.9 Hz), 6.11 (dd, 1H, J = 5.2 Hz, 3.4 Hz), 6.02 (t, 1H, J = 5.4 Hz), 4.83–4.81 (m, 2H), 4.64 (dd, 1H, J = 13.5 Hz, 4.9 Hz), 3.90 (s, 3H). ^{13}C NMR (126 MHz, $CDCl_3$) δ (ppm) 166.23, 165.20, 165.04, 161.53, 144.38, 136.04, 133.90, 133.78, 133.51, 129.97, 129.87, 129.84, 129.37, 128.79, 128.72, 128.65, 128.60, 92.60, 80.96, 75.30, 71.33, 63.54, 61.47, 53.50, 52.23. ESI-MS (positive) for $C_{31}H_{25}N_2O_9INa$ ($[M + Na]^+$): calcd, 719.05; found, 718.97.

Methyl 4-Propynyl-1-(2′,3′,5′-tribenzoyl-β-D-ribofuranosyl)pyrazole-3-carboxylate (6b). To a solution of 223 mg (0.321 mmol) of **6a**, 9.8 mg (0.051 mmol) of CuI, and 18.5 mg (0.016 mmol) of tetrakis(triphenylphosphine)palladium(0) in 1.6 mL of dry CH_3CN were added 67 μL (0.481 mmol) of triethylamine and 146 μL (0.481 mmol) tributyl(1-propynyl)tin under argon atmosphere, and the solution was stirred at room temperature for 8 h. The reaction mixture was then partitioned with EtOAc/H_2O, and the organic layer was washed three times with saturated NaCl aqueous solution, dried over Na_2SO_4, filtrated, and evaporated. An amount of 146 mg (0.24 mmol, 75%) of **6b** was obtained by silica gel column chromatography (solvent, *n*-hexane/EtOAc = 4: 1 (v/v)). ^{1}H NMR (500 MHz, $CDCl_3$) δ (ppm) 8.06 (d, 2H, J = 7.5 Hz), 7.97 (d, 2H, J = 7.5 Hz), 7.91 (d, 2H, J = 6.9 Hz), 7.80 (s, 1H), 7.58–7.53 (m, 3H), 7.44 (t, 2H, J = 7.7 Hz), 7.40 (t, 2H, J = 8.0 Hz), 7.35 (t, 2H, J = 8.0 Hz), 6.22 (d, 1H, J = 2.9 Hz), 6.11 (dd, 1H, J = 5.2 Hz, 3.4 Hz), 6.02 (t, 1H, J = 5.4 Hz), 4.83–4.77 (m, 2H), 4.64 (dd, 1H, J = 12.0, 4.0 Hz), 3.91 (s, 3H), 2.04 (s, 3H). ^{13}C NMR (126 MHz, $CDCl_3$) δ (ppm) 166.27, 165.19, 165.00, 161.64, 144.42, 133.85, 133.74, 133.36, 132.92, 129.96, 129.88, 129.44, 128.76, 128.66, 128.63, 128.57, 108.21, 92.45, 90.18, 80.78, 75.29, 71.31, 68.91, 63.68, 52.17, 4.67. HR-MS (ESI-positive) for $C_{34}H_{28}N_2O_9Na$ ($[M + Na]^+$): calcd, 631.1687; found, 631.1705.

Methyl 4-Phenylethynyl-1-(2′,3′,5′-tribenzoyl-β-D-ribofuranosyl)pyrazole-3-carboxylate (6c). 6c was synthesized in a similar procedure to **6b** by the palladium-catalyzed coupling reaction. To a solution of 491 mg (0.705 mmol) of **6a**, 21.5 mg (0.113 mmol) of CuI, and 40.7 mg (0.035 mmol) of tetrakis(triphenylphosphine)-palladium(0) in 3.5 mL of dry CH_3CN were added 147 μL (1.06 mmol) of triethylamine and 116 μL (1.06 mmol) ethynylbenzene under argon atmosphere, and the solution was stirred at room temperature for 9 h. Work-up was carried out as described above. An amount of 368 mg (0.548 mmol, 78%) of **6c** was obtained by silica gel column chromatography (solvent, *n*-hexane/EtOAc = 4:1 (v/v)). ^{1}H NMR (500 MHz, $CDCl_3$) δ (ppm) 8.08 (d, 2H, J = 7.5 Hz), 7.98 (d, 2H, J = 7.5 Hz), 7.94 (s, 1H), 7.92 (d, 2H, J = 7.5 Hz), 7.59–7.33 (m, 14H), 6.27 (d, 1H, J = 3.4 Hz), 6.15 (dd, 1H, J = 5.0, 3.6 Hz), 6.05 (t, 1H, J = 5.7 Hz), 4.86–4.81 (m, 2H), 4.66 (dd, 1H, J = 11.7, 3.7 Hz), 3.94 (s, 3H). ^{13}C NMR (126 MHz, $CDCl_3$) δ (ppm) 166.28, 165.19, 165.02, 161.44, 144.69, 133.88, 133.76, 133.45, 132.84, 131.69, 129.98, 129.88, 129.86, 129.41, 128.71, 128.65, 128.59, 128.48, 128.37, 123.18, 107.53, 93.40, 92.57, 80.89, 78.95, 75.35, 71.27, 63.58, 52.24. HR-MS (ESI-positive) for $C_{39}H_{30}N_2O_9Na$ ($[M + Na]^+$): calcd, 693.1844; found, 693.1866.

General Procedure for Ammonia Treatment of Protected Nucleoside (6a−c). Ammonia treatment of protected nucleoside **6a−c** converts the 3-carboxylate group to the 3-carboxiamide group as well as benzoyl-protected 2′-, 3′-, and 5′-hydroxyl groups to free hydroxyl groups. The protected nucleosides were dissolved in 10 mL of saturated (~7 N) ammonia in methanol (Sigma-Aldrich) and stirred at room temperature overnight. Ammonia and solvent were removed under reduced pressure, and deprotected nucleosides **7a−c** were purified by a silica gel column chromatography (solvent, 0−10% methanol in CH_2Cl_2) followed by preparative HPLC purification.

4-Iodo-1-β-D-ribofuranosylpyrazole-3-carboxamide (7a). An amount of 319 mg (0.458 mmol) of **6a** was treated with ammonia as described above. Following silica gel column chromatography, **7a** was purified by two-step HPLC purifications: first, HPLC condition I (see General Procedures); second, 5% (v/v) CH_3CN in H_2O isocratic conditions (flow rate 10 mL/min). Yield, 82.8 mg (0.224 mmol, 49%). ^{1}H NMR (500 MHz, DMSO-d_6) δ (ppm) 8.22 (s, 1H), 7.46 (bs, 1H), 7.27 (bs, 1H), 5.61 (d, 1H, J = 4.6 Hz), 5.43 (d, 1H, J = 5.7 Hz), 5.08 (d, 1H, J = 5.7 Hz), 4.89 (t, 1H, J = 5.7 Hz), 4.28 (q, 1H, J = 5.0 Hz), 4.07 (q, 1H, J = 5.0 Hz), 3.87 (q, 1H, J = 4.4 Hz), 3.61–3.56 (m, 1H), 3.49–3.45 (m, 1H). ^{13}C NMR (126 MHz, DMSO-d_6) δ (ppm) 163.12, 145.45, 137.13, 94.48, 85.97, 75.15, 70.64, 61.83, 59.22. HR-

MS (ESI-positive) for $C_9H_{12}N_3O_5INa$ ($[M + Na]^+$): calcd, 391.9714; found, 391.9702.

4-Propynyl-1-β-D-ribofuranosylpyrazole-3-carboxamide (7b). An amount of 128 mg (0.211 mmol) of **6b** was treated with ammonia as described above. Following silica gel column chromatography, **7b** was purified by two-step HPLC purifications, first, HPLC condition I (see General Procedures); second, 10% (v/v) CH_3CN in H_2O isocratic conditions (flow rate 10 mL/min). Yield, 35.7 mg (0.127 mmol, 60%). ^{1}H NMR (500 MHz, DMSO-d_6) δ (ppm) 8.22 (s, 1H), 7.31 (bs, 1H), 7.28 (bs, 1H), 5.59 (d, 1H, J = 4.0 Hz), 5.44 (d, 1H, J = 5.7 Hz), 5.07 (d, 1H, J = 5.2 Hz), 4.89 (t, 1H, J = 5.4 Hz), 4.25 (q, 1H, J = 5.0 Hz), 4.07 (q, 1H, J = 5.2 Hz), 3.87 (q, 1H, J = 4.4 Hz), 3.61–3.57 (m, 1H), 3.49–3.45 (m, 1H), 1.96 (s, 3H). ^{13}C NMR (126 MHz, DMSO-d_6) δ (ppm) 162.72, 146.67, 134.57, 104.04, 94.38, 88.81, 85.86, 75.21, 71.12, 70.56, 61.78, 4.71. HR-MS (ESI-positive) for $C_{12}H_{16}N_3O_5$ ($[M + H]^+$): calcd, 282.1084; found, 282.1090. HR-MS (ESI-positive) for $C_{12}H_{15}N_3O_5Na$ ($[M + Na]^+$): calcd, 304.0904; found, 304.0898.

4-Phenylethynyl-1-β-D-ribofuranosylpyrazole-3-carboxamide (7c). An amount of 359 mg (0.535 mmol) of **6c** was treated with ammonia as described above. Following silica gel column chromatography, **7c** was purified by two-step HPLC purifications: first, HPLC condition I (see General Procedures); second, 28% (v/v) CH_3CN in H_2O isocratic condition (flow rate 10 mL/min). Yield, 137 mg (0.398 mmol, 74%). ^{1}H NMR (500 MHz, DMSO-d_6) δ (ppm) 8.40 (s, 1H), 7.45–7.34 (m, 7H), 5.64 (d, 1H, J = 4.0 Hz), 5.48 (d, 1H, J = 5.7 Hz), 5.10 (d, 1H, J = 5.2 Hz), 4.92 (t, 1H, J = 5.7 Hz), 4.30 (q, 1H, J = 5.0 Hz), 4.10 (q, 1H, J = 5.0 Hz), 3.90 (q, 1H, J = 4.4 Hz), 3.64–3.59 (m, 1H), 3.52–3.48 (m, 1H). ^{13}C NMR (126 MHz, DMSO-d_6) δ (ppm) 162.64, 147.07, 134.80, 131.62, 129.23, 128.98, 123.42, 103.25, 94.53, 91.66, 85.99, 81.59, 75.28, 70.57, 61.79. HR-MS (ESI-positive) for $C_{17}H_{18}N_3O_5$ ($[M + H]^+$): calcd, 344.1241; found, 344.1245. HR-MS (ESI-positive) for $C_{17}H_{17}N_3O_5Na$ ($[M + Na]^+$): calcd, 366.1060; found, 366.1065.

General Procedure for the Synthesis of Nucleoside 5′-Triphosphates (8, 9a−c). The 0.1 mmol scale synthesis of 5′-triphosphates of ribavirin (**1**) and its analogues (**7a−c**) and DEAE Sephadex A-25 column purification were carried out as described by Kimoto et al.[13] HPLC purification following the DEAE column provides pure triphosphates. The yield and the molar absorption coefficient (ε) of these triphosphates at pH 7.0 were determined by quantitative analysis of the phosphorus in these compounds.[13]

Ribavirin 5′-Triphoshate (8). HPLC purification: HPLC condition II (see General Procedures), detection; UV 220 nm. Yield, 28%. ^{1}H NMR (500 MHz, D_2O) δ (ppm) 8.72 (s, 1H), 5.93 (d, 1H, J = 4.6 Hz), 4.64–4.61 (m, 1H), 4.49 (t, 1H, J = 4.9 Hz), 4.30–4.29 (m, 1H), 4.15–4.12 (m, 2H), 3.10 (q, 18H, J = 7.3 Hz), 1.18 (t, 27H, J = 7.2 Hz). ^{31}P NMR (202 MHz, D_2O) δ (ppm) −9.44 (d, 1H, J = 18.6 Hz), −10.26 (d, 1H, J = 18.6 Hz), −21.78 (t, 1H, J = 19.4 Hz). HR-MS (ESI-negative) for $C_8H_{14}N_4O_{14}P_3$ ($[M - H]^-$): calcd, 482.9714; found, 482.9724. UV–vis spectrum (in 10 mM sodium phosphate buffer, pH 7.0): no λ_{max} was observed over the range 220−400 nm ($\varepsilon_{220} = 7.1 \times 10^3$).

4-Iodo-1-β-D-ribofuranosylpyrazole-3-carboxamide 5′-Triphosphate (9a). HPLC purification: HPLC condition II (see General Procedures); detection, UV 250 nm. Yield, 27%. ^{1}H NMR (500 MHz, D_2O) δ (ppm) 8.08 (s, 1H), 5.76 (d, 1H, J = 5.2 Hz), 4.64–4.59 (m, 1H), 4.45 (t, 1H, J = 4.6 Hz), 4.26–4.25 (m, 1H), 4.11–4.10 (m, 2H), 3.10 (q, 18H, J = 7.3 Hz), 1.18 (t, 27H, J = 7.5 Hz). ^{31}P NMR (202 MHz, D_2O) δ (ppm) −9.36 (d, 1H, J = 18.6 Hz), −10.24 (d, 1H, J = 17.1 Hz), −21.70 (t, 1H, J = 19.4 Hz). HR-MS (ESI-negative) for $C_9H_{14}N_3O_{14}IP_3$ ($[M - H]^-$): calcd, 607.8728; found, 607.8724. UV–vis spectrum (in 10 mM sodium phosphate buffer, pH 7.0), λ_{max} = 250 nm ($\varepsilon_{250} = 3.0 \times 10^3$).

4-Propynyl-1-β-D-ribofuranosylpyrazole-3-carboxamide 5′-Triphosphate (9b). HPLC purification: HPLC condition II (see General Procedures); detection, UV 260 nm. Yield, 20%. ^{1}H NMR (500 MHz, D_2O) δ (ppm) 8.04 (s, 1H), 5.74 (d, 1H, J = 5.7 Hz), 4.61–4.58 (m, 1H), 4.44 (t, 1H, J = 4.6 Hz), 4.26–4.25 (m, 1H), 4.11–4.10 (m, 2H), 3.10 (q, 18H, J = 7.3 Hz), 1.94 (s, 3H), 1.18 (t, 27H, J = 7.2 Hz). ^{31}P NMR (202 MHz, D_2O) δ (ppm) −9.38 (d, 1H, J = 18.6 Hz), −10.21 (d, 1H, J = 20.1 Hz), −21.73 (t, 1H, J = 20.9 Hz). HR-MS (ESI-negative) for $C_{12}H_{17}N_3O_{14}P_3$ ($[M - H]^-$): calcd, 519.9918; found, 519.9920. UV–vis spectrum (in 10 mM sodium phosphate buffer, pH 7.0), λ_{max} = 262 nm ($\varepsilon_{262} = 3.4 \times 10^3$).

4-Phenylethynyl-1-β-D-ribofuranosylpyrazole-3-carboxamide 5′-Triphosphate (9c). HPLC purification: HPLC condition III (see General Procedures); detection, UV 271 nm. Yield, 7%. ^{1}H NMR (500 MHz, D_2O) δ (ppm) 8.18 (s, 1H), 7.52–7.50 (m, 2H), 7.36–7.35 (m, 3H), 5.80 (d, 1H, J = 5.2 Hz), 4.63–4.59 (m, 1H), 4.48 (t, 1H, J = 4.6 Hz), 4.28–4.27 (m, 1H), 4.14–4.13 (m, 2H), 3.10 (q, 18H, J = 7.3 Hz), 1.18 (t, 27H, J = 7.5 Hz). ^{31}P NMR (202 MHz, D_2O) δ (ppm) −8.72 (bs, 1H), −10.09 (d, 1H, J = 18.6 Hz), −21.25 (bs, 1H). HR-MS (ESI-negative) for $C_{17}H_{19}N_3O_{14}P_3$ ($[M - H]^-$): calcd, 582.0074; found, 582.0070. UV–vis spectrum (in 10 mM sodium phosphate buffer, pH 7.0), λ_{max} = 272 nm ($\varepsilon_{272} = 1.9 \times 10^4$).

Expression and Purification of 3D^{pol}. Expression and purification of 3D^{pol} were performed as described previously.[14] A single band of 3D^{pol} on SDS−PAGE was obtained. The concentration of purified 3D^{pol} was determined with BCA protein assay kit (PIERCE). Purified 3D^{pol} was stored at −70 °C in 50 mM HEPES−KOH, pH 7.5, 5 mM $MgCl_2$, 20% glycerol, 0.1% NP-40, and 1 mM DTT.

Preparation of Oligonucleotides for 3D^{pol} Assay. Sym/sub-U and sym/sub-C (Figure 3)[7] were used as template primer for 3D ^{pol} assay. These 10-mer RNA oligonucleotides purchased from Greiner Bio-One were further purified on denaturing PAGE (200 mm × 400 mm × 2 mm, 20% polyacrylamide containing 7 M urea). The concentrations of purified oligonucleotides were determined from UV absorbance at 260 nm (TE buffer).

5′-^{32}P-Labeling of Oligonucleotides. Temperature of all enzymatic reactions was controlled in Thermal Cycler Dice Gradient (TaKaRa). An amount of 0.1 nmol of sym/sub oligonucleotide was mixed with 5 μCi [γ-^{32}P]ATP (GE Healthcare) and 10 U of T4 polynucleotide kinase (TaKaRa) in provided T4 PNK buffer (total volume is 10 μL) and incubated at 37 °C for 1 h. After addition of 30 μL of H_2O, labeled oligonucleotide was separated from unreacted [γ-^{32}P]ATP by a MicroSpin G-25 column (GE Healthcare). Labeled oligonucleotide was then diluted to one-tenth by mixing 0.9 nmol of unlabeled oligonucleotide. H_2O was added to the total volume of 100 μL (final concentration of oligonucleotide was 10 μM).

3D^{pol} Assays. 3D^{pol} assays were carried out according to literatures.[15,16] Ultrapure ATP and GTP were purchased from GE Healthcare and used without further purification. Prior to preparing the reaction mixture of 3D^{pol} assays, sym/sub oligonucleotide was annealed by heating to 90 °C for 1 min and cooled slowly (5 °C/min) to 10 °C. 3D^{pol} was diluted to 12.5 μM immediately prior to use in 50 mM HEPES−KOH, pH 7.5, 10 mM 2-mercaptoethanol, 5 mM $MgCl_2$, 60 μM $ZnCl_2$, and 20% glycerol. For time course experiments, reaction mixture of 50 mM HEPES−KOH, pH 7.5, 10 mM 2-mercaptoethanol, 5 mM $MgCl_2$, 60 μM $ZnCl_2$, 20 U of RNase inhibitor (Promega), 500 μM NTP, 5 pmol of ^{32}P-labeled sym/sub, and 1.25 μM 3D^{pol} in a total volume of 10 μL was incubated at 30 °C. The reaction was quenched at each time point by adding 1 μL of 0.5 M EDTA. For steady-state kinetics, reaction mixture of 50 mM HEPES−KOH, pH 7.5, 10 mM 2-mercaptoethanol, 5 mM $MgCl_2$, 60 μM $ZnCl_2$, 10 U of RNase inhibitor, 10−250 μM NTP, 2.5 pmol of ^{32}P-labeled sym/sub, and 1.25 μM 3D^{pol} in a total volume of 5 μL was incubated at 30 °C for 2 min. Reaction was quenched by adding 0.5 μL of 0.5 M EDTA.

Denaturing PAGE Analysis of 3D^{pol} Products. To each reaction mixture was added an equal volume of loading buffer (90% formamide, 0.025% bromophenol blue, and 0.025% xylene cyanol). After the mixture was heated at 70 °C for 5 min, one-fourth of the total amount was loaded onto 20% denaturing polyacrylamide gel (200 mm × 400 mm × 0.5 mm, 7 M urea). Electrophoresis was carried out in 1× TBE at 40 W. Bands were visualized and quantitated by Personal Molecular Imager FX with Quantity One software (Bio-Rad).

Antiviral Evaluation. HeLa S3 cells were maintained in DMEM/F-12 supplemented with 2% dialyzed fetal bovine serum and penicillin/streptomycin (1×, Invitrogen). Nucleosides were freshly suspended in 100% DMSO (200 mM) immediately prior to use. Infection with poliovirus (PV) employed HeLa S3 host cells (1×10^5) plated 1 day prior to treatment in 24-well plates. Cells were pretreated by addition of nucleoside at the specified concentration in fresh media adjusted to a final concentration of 1% DMSO. After a 1 h of incubation at 37 °C, the medium was removed and cells were infected with PV (1×10^6 PFU) in phosphate-buffered saline (PBS, total volume of 0.1 mL). Plates were incubated for 15 min at 23 °C. PBS was removed by aspiration, and a fresh, prewarmed (37 °C) medium containing the specified amount of nucleoside was added. The infection was allowed to proceed at 37 °C for 6 h. Cells were washed with PBS and collected after treatment with trypsin. Cells were pelleted by centrifugation, resuspended in PBS (0.5 mL), and subjected to three freeze–thaw cycles. Cell debris was removed by centrifugation, and the supernatant containing the cell-associated virus was saved. Titer was determined by applying serial dilutions of supernatant to HeLa S3 monolayers (plated in six-well plates 1 day earlier at 5×10^5 cells/well) and overlaying with growth medium containing 1% low-melting point agarose. Plates were incubated for 2 days at 37 °C, at which time the agar was removed and plaques were visualized by staining with crystal violet (1%) in aqueous ethanol (20%).

Acknowledgment. We gratefully acknowledge the NIH (Grant AI054776 to C.E.C.) for financial support.

Supporting Information Available: ^{1}H NMR spectra of **1**, **7a**, **7b**, and **7c**. This material is available free of charge via the Internet at http://pubs.acs.org.

References

(1) Sidwell, R. W.; Huffman, J. H.; Khare, G. P.; Allen, L. B.; Witkowski, J. T.; Robins, R. K. Broad-Spectrum Antiviral Activity of Virazole: 1-β-D-Ribofuranosyl-1,2,4-triazole-3-carboxamide. *Science* **1972**, *177*, 705–706.

(2) Witkowski, J. T.; Robins, R. K.; Sidwell, R. W.; Simon, L. N. Design, Synthesis, and Broad Spectrum Antiviral Activity of 1-β-D-ribofuranosyl-1,2,4-triazole-3-carboxamide and Related Nucleosides. *J. Med. Chem.* **1972**, *15*, 1150–1154.

(3) Streeter, D. G.; Witkowski, J. T.; Khare, G. P.; Sidwell, R. W.; Bauer, R. J.; Robins, R. K.; Simon, L. N. Mechanism of Action of 1-β-D-Ribofuranosyl-1,2,4-triazole-3-carboxamide (Virazole), a New Broad-Spectrum Antiviral Agent. *Proc. Natl. Acad. Sci. U.S.A.* **1973**, *70*, 1174–1178.

(4) Leyssen, P.; Balzarini, J.; De Clercq, E.; Neyts, J. The Predominant Mechanism by Which Ribavirin Exerts Its Antiviral Activity in Vitro against Flaviviruses and Paramyxoviruses Is Mediated by Inhibition of IMP Dehydrogenase. *J. Virol.* **2005**, *79*, 1943–1947.

(5) Wray, S. K.; Smith, R. H.; Gilbert, B. E.; Knight, V. Effects of Selenazofurin and Ribavirin and Their 5′-Triphosphates on Replicative Functions of Influenza A and B Viruses. *Antimicrob. Agents Chemother.* **1986**, *29*, 67–72.

(6) Kentsis, A.; Topisirovic, I.; Culjkovic, B.; Shao, L.; Borden, K. L. B. Ribavirin Suppresses eIF4E-Mediated Oncogenic Transformation by Physical Mimicry of the 7-Methylguanosine mRNA Cap. *Proc. Natl. Acad. Sci. U.S.A.* **2004**, *101*, 18105–18110.

(7) Crotty, S.; Maag, D.; Arnold, J. J.; Zhong, W.; Lau, J. Y.; Hong, Z.; Andino, R.; Cameron, C. E. The Broad-Spectrum Antiviral Ribonucleoside Ribavirin Is an RNA Virus Mutagen. *Nat. Med.* **2000**, *6*, 1375–1379.

(8) Crotty, S.; Cameron, C. E.; Andino, R. RNA Virus Error Catastrophe: Direct Molecular Test by Using Ribavirin. *Proc. Natl. Acad. Sci. U.S.A.* **2001**, *98*, 6895–6900.

(9) Vignuzzi, M.; Stone, J. K.; Andino, R. Ribavirin and Lethal Mutagenesis of Poliovirus: Molecular Mechanism, Resistance and Biological Implications. *Virus Res.* **2005**, *107*, 173–181.

(10) Mitsui, T.; Kimoto, M.; Sato, A.; Yokoyama, S.; Hirao, I. An Unnatural Hydrophobic Base, 4-Propynylpyrrole-2-carboaldehyde, as an Efficient Pairing Partner of 9-Methylimidazo[(4,5)-*b*]pyridine. *Bioorg. Med. Chem. Lett.* **2003**, *13*, 4515–4518.

(11) Castanet, A.-S.; Colobert, F.; Broutin, P.-E. Mild and Regioselective Iodination of Electron-Rich Aromatics with *N*-Iodosuccinimide and Catalytic Trifluoroacetic Acid. *Tetrahedron Lett.* **2002**, *43*, 5047–5048.

(12) Manfredini, S.; Bazzanini, R.; Baraldi, P. G.; Guarneri, M.; Simoni, D.; Marongiu, M. E.; Pani, A.; Tramontano, E.; La Colla, P. Pyrazole-Related Nucleosides. Synthesis and Antiviral/Antitutor Activity of Some Substituted Pyrazole and Pyrazole[4,3-*d*]-1,2,3-triazin-4-one Nucleosides. *J. Med. Chem.* **1992**, *35*, 917–924.

(13) Kimoto, M.; Endo, M.; Mitsui, T.; Okuni, T.; Hirao, I.; Yokoyama, S. Site-Specific Incorporation of a Photo-Crosslinking Component into RNA by T7 Transcription Mediated by Unnatural Base Pairs. *Chem. Biol.* **2004**, *11*, 47–55.

(14) Gohara, D. W.; Ha, C. S.; Ghosh, S. K. B.; Arnold, J. J.; Wisniewski, T. J.; Cameron, C. E. Production of "Authentic" Poliovirus RNA-Dependent RNA Polymerase ($3D^{pol}$) by Ubiquitin-Protease-Mediated Cleavage in *Escherichia coli*. *Protein Expression Purif.* **1999**, *17*, 128–138.

(15) Arnold, J. J.; Ghosh, S. K. B.; Cameron, C. E. Poliovirus RNA-Dependent RNA Polymerase ($3D^{pol}$). Divalent Cation Modulation of Primer, Template, and Nucleotide Selection. *J. Biol. Chem.* **1999**, *274*, 1285–1288.

(16) Arnold, J. J.; Cameron, C. E. Poliovirus RNA-Dependent RNA Polymerase ($3D^{pol}$). Assembly of Stable, Elongation-Competent Complexes by Using a Symmetrical Primer-Template Substrate (Sym/sub). *J. Biol. Chem.* **2000**, *275*, 5329–5336.

(17) Harki, D. A.; Graci, J. D.; Korneeva, V. S.; Ghosh, S. K. B.; Hong, Z.; Cameron, C. E.; Peterson, B. R. Synthesis and Antiviral Evaluation of a Mutagenic and Non-Hydrogen Bonding Ribonucleoside Analogue: 1-β-D-Ribofuranosyl-3-nitropyrrole. *Biochemistry* **2002**, *41*, 9026–9033.

(18) Huttel, R.; Schafer, O.; Jochum, P. The Iodination of Pyrazole. *Ann. Chem.* **1955**, *593*, 200–207.

(19) Moriyama, K.; Kimoto, M.; Mitsui, T.; Yokoyama, S.; Hirao, I. Site-specific biotinylation of RNA molecules by transcription using unnatural base pairs. *Nucleic Acids Res.* **2005**, *33*, e129.

(20) Arnold, J. J.; Vignuzzi, M.; Stone, J. K.; Andino, R.; Cameron, C. E. Remote Site Control of an Active Site Fidelity Checkpoint in a Viral RNA-Dependent RNA Polymerase. *J. Biol. Chem.* **2005**, *280*, 25706–25716.

(21) Beese, L. S.; Friedman, J. M.; Steitz, T. A. Crystal Structures of the Klenow Fragment of DNA Polymerase I Complexed with Deoxynucleoside Triphosphate and Pyrophosphate. *Biochemistry* **1993**, *32*, 14095–14101.

(22) Thompson, A. A.; Peersen, O. B. Structural Basis for Proteolysis-Dependent Activation of the Poliovirus RNA Dependent RNA Polymerase. *EMBO J.* **2004**, *23*, 3462–3471.

(23) Thompson, A. A.; Albertini, R. A.; Peersen, O. B. Stabilization of Poliovirus Polymerase by NTP Binding and Fingers−Thumb Interactions. *J. Mol. Biol.* **2007**, *366*, 1459–1474.

(24) Inamoto, N.; Masuda, S. Revised Method for Calculation of Group Electronegativities. *Chem. Lett.* **1982**, *11*, 1003–1006.

(25) Wu, J. Z.; Larson, G.; Walker, H.; Shim, J. H.; Hong, Z. Phosphorylation of Ribavirin and Viramidine by Adenosine Kinase and Cytosolic 5′-Nucleotidase II: Implications for Ribavirin Metabolism in Erythrocytes. *Antimicrob. Agents Chemother.* **2005**, *49*, 2164–2171.

JM7009952